Identifying Ca^{2+}-Binding Sites in Proteins by Liquid Chromatography-Mass Spectrometry Using Ca^{2+}-Directed Dissociations

Azadeh Jamalian‡§‡‡, Evert-Jan Sneekes‡§‡‡, Hans Wienk¶, Lennard J. M. Dekker‡, Paul J. A. Ruttink‖, Mario Ursem§, Theo M. Luider‡, and Peter C. Burgers‡**

Here we describe a new method to identify calcium-binding sites in proteins using high-resolution liquid chromatography-mass spectrometry in concert with calcium-directed collision-induced dissociations. Our method does not require any modifications to the liquid chromatography-mass spectrometry apparatus, uses standard digestion protocols, and can be applied to existing high-resolution MS data files. In contrast to NMR, our method is applicable to very small amounts of complex protein mixtures (femtomole level). Calcium-bound peptides can be identified using three criteria: (1) the calculated exact mass of the calcium containing peptide; (2) specific dissociations of the calcium-containing peptide from threonine and serine residues; and (3) the very similar retention times of the calcium-containing peptide and the free peptide. ***Molecular & Cellular Proteomics 13: 10.1074/mcp.M114.038182, 3177–3183, 2014.***

Calcium-dependent protein interactions mostly organized in protein networks are responsible for the regulation of cell cycle progression, cell growth, differentiation, secretion, and cytoskeletal organization (1–3). As many of these proteins are linked to various pathological conditions, they are clinically important. The speed at which calcium can have an interplay between various cellular components is impressive and comes notably detectable in neurological processes and in muscle contraction. Calcium binding sites in proteins can be determined by NMR spectroscopy (4, 5). For example, by such NMR measurements, the Ca^{2+}-binding sites of the tellurite-resistance protein TerD from *Klebsiella pneumoniae* were found to be formed in part by a highly conserved motif of 13 residues specified by the sequence GDN(R/L)TG(E/A)GDGDDE (4).

Although NMR is the gold standard to study calcium binding in proteins, this approach has several drawbacks. For instance, protein size is limited ($<$ 30 kDa) and proteins should be pure and isotopically labeled. In addition, although the information content is high, NMR is relatively insensitive compared with other techniques such as MS and fluorescence spectroscopy, and relatively large quantities of material (typically 0.5 ml at 0.5–1.0 mM in biological samples) are needed, although efforts are devoted to improve sensitivity in NMR, such as stripline NMR (6).

In bottom-up proteomics, proteolytic peptides, generated by enzymatic digestion of complex protein mixtures, are sequenced by MS-based methods (MS/MS (7, 8)) using collision-induced dissociations. Because of the even higher complexity of these peptide mixtures, liquid chromatography (LC)[1] is used to separate the peptides prior to sequencing. In such an LC-MS/MS procedure, many peptides can be identified belonging to the same protein. It has been stated (9) that by this procedure more peptides are analyzed than strictly necessary for identification purposes, but it can equally well be argued that such large coverages enable more reliable protein identifications; moreover, these larger coverages allow the detection of post-translational modifications, including specific calcium complexation as described here.

Considering the need of identifying calcium-bound proteins in complex biological samples at low concentrations, we set out to develop a novel method for detecting Ca^{2+}-binding sites in proteins based on LC-MS.

EXPERIMENTAL PROCEDURES

All peptide samples were prepared as 0.01 M in water. The matrix-assisted laser desorption/ionization (MALDI) matrix α-cyano-4-hydroxycinnamic acid (CHCA) was prepared as 0.01 M in acetonitrile/water, 50:50 (v/v). Following the procedure of Ruttink *et al.* (10), the ethanolamine and ethanolamine-d_4 solution was mixed with the metal formate or metal acetate solution and with the matrix solution in a

From the ‡Department of Neurology, Laboratory of Neuro-Oncology, Erasmus Medical Center, P.O. Box 2040, 3000 CA, Rotterdam, The Netherlands; §Thermo Fisher Scientific/Dionex, Abberdaan 114, 1046 AA, Amsterdam, The Netherlands; ¶NMR Spectroscopy, Bijvoet Center for Biomolecular Research, P.O. Box 80.075, 3508 TB, Utrecht University, Utrecht, The Netherlands; ‖Theoretical Chemistry Group, University of Utrecht, 3508 TC, Utrecht, The Netherlands

Received January 29, 2014, and in revised form, July 7, 2014
Published, MCP Papers in Press, July 14, 2014, DOI 10.1074/mcp.M114.038182
Author contributions: A.J., E.S., L.J.D., M.U., T.M.L., and P.C.B. designed research; A.J., E.S., H.W., L.J.D., P.J.R., and P.C.B. performed research; A.J., E.S., H.W., L.J.D., P.J.R., M.U., T.M.L., and P.C.B. analyzed data; A.J., E.S., T.M.L., and P.C.B. wrote the paper.

[1] The abbreviations used are: LC, liquid chromatography; MALDI, matrix-assisted laser desorption/ionization; CID, collision-induced dissociation; ESI, electrospray ionization.

ratio of 1:1:1 (v/v/v), and 1 μl of this mixture was spotted on a graphite surface. MALDI-TOF and TOF/TOF mass spectra were recorded on a Bruker Ultraflex III mass spectrometer, Bremen, Germany (11). MS spectra were recorded using a random laser walk and threshold laser fluence until 5,000 single laser shot mass spectra were accumulated. Fragmentation efficiency curves were obtained on a Bruker Apex IV MALDI-FT-ICR mass spectrometer. For these measurements, 2,5-dihydroxy benzoic acid instead of CHCA was used as the matrix (12). The ratio of product ion/precursor ion was measured as a function of the laboratory collision energy (E_{lab}) with subsequent transformation to the center-of-mass framework (E_{com}) according to: $E_{com} = [N/(M+N)]E_{lab}$ where M is the precursor ion mass and N the mass of the collision gas (13). ESI mass spectra and MS/MS spectra were obtained by direct infusion of the ethanolamine samples and the calcium acetate or formate solution mixtures diluted with an equal volume of isopropanol using a Bruker Esquire ESI-Iontrap mass spectrometer with the following settings: capillary voltage 4000V, octapole RF 40Vpp, and trap drive 30. Infusion rate was 240 μl/h.

Ab initio calculations were performed using standard density functional theory calculations with the Gaussian03 suite of programs (14). Geometry optimizations and vibrational frequencies were obtained using the B3LYP exchange-correlation potential (15, 16) with the 6–311G(2d,d,p) (CBSB7) basis set.

LC-Orbitrap measurements were performed as described previously (17). The onco-neural protein HuD was recombinantly produced, isolated, and purified as described previously (18) and was subjected to digestion as follows: A 50 μl aliquot containing 1 mg/ml HuD in 10 mM of HEPES buffer, pH = 8.2, in 8 M urea was purified through a Zeba™, Thermo Scientific, Rockford, IL desalt column, equilibrated with 50 mM of ammonium bicarbonate. In a heat block, 50 μl of 0.5 M dithiotreitol (in H_2O) were incubated at 60 °C for 30 min at 400 rpm. Subsequently, 2.5 μl of iodoacetic acid 0.3 M was then added to the sample and left for 30 min in the dark. Finally, 5 μl MS-grade porcine modified trypsin gold (Promega, Madison, WI) with a concentration of 0.1 μg/μl, 940 μl H_2O, and 60 μl Tris buffer- HCl (pH = 8.8) was added and incubated overnight at 37 °C at 400 rpm.

Calcyclin sample was prepared as follows: 500 μl of TBS (20 mM Tris, 50 mM NaCl, pH 8.0) were added to the lyophilized 100 μg vial of human S100 calcium-binding protein A6, commercially purchased from ADIPOBIOSCIENCE, Santa Clara, CA (code: 00316–01-100, lot no. 000205, protein Id: Swiss P06703, Gene ID: 6277, MW: 12kD, Source: *Escherichia coli*, purity: >95%). A stock solution of 200 μg/ml was achieved and allowed to set at least 30 min at 4 °C and mixed well afterward. A solution of 1 pmol/μl of the calcyclin sample was used for the LC-MS/MS experiments.

NMR experiments on the synthesized and pure GTNYDEG peptide were performed at 298 K on a Bruker Avance III 600 MHz spectrometer equipped with a 5 mm TXI probe head. NMR samples contained 1 mM peptide in 10% D_2O/H_2O in the absence and presence of 10% of 10 mM of calcium formate.

RESULTS

During a mass spectrometric quality assessment (by high-resolution matrix-assisted laser desorption/ionization-Fourier transform-ion cyclotron resonance-mass spectrometry, MALDI-FTICR-MS) of synthetic 15-mer peptides derived from the onco-neural protein HuD, we noticed (19) that certain peptide motifs such as TNYDEA displayed an extraordinary large affinity toward Ca^{2+} as could be distinguished by high-resolution MS (supplemental Fig. S1). This was evident from intense peaks corresponding to $[P - H + Ca]^+$, present at 37.9470 Da higher than that for the protonated peptide $[P + H]^+$ as opposed to the usually found lesser intense peaks 37.9559 Da higher for the K^+ adducts corresponding to $[P + K]^+$. The mass difference, 8.9 mDa is easily detected on an FTICR instrument with a resolution of 100,000 (full width at the half height, FWHH). After purification of the peptide by preparative LC, the calcium-containing peptide was still present (supplemental Fig. S1*B*) attesting to the strong binding of calcium. From the high-resolution MS/MS spectra (supplemental Fig. S2), it became also evident that when a threonine (T) is present, the $[P - H + Ca]^+$ loses 44.0262 Da, corresponding to loss of acetaldehyde, whereas at the same collision energy the $[P + K]^+$ ions do not show any such loss. When more T residues are present, sequential losses of CH_3CHO are observed. Such acetaldehyde loss is also observed as sequential fragmentation from intense product ions, such as from the b-type aspartic acid product ions. When a serine (S) is present, loss of 30.0106, corresponding to loss of $CH_2 = O$, is observed. Such losses are also observed in electrospray ionization (supplemental Fig. S2*B*) showing that the calcium-containing peptide is also detectable under ESI conditions. T and S (and also tyrosine, Y) residues, which are present together with the acidic amino acid residues aspartic acid (D) and glutamic acid (E) in the 15-mer peptides studied in Ref. 16, all contain hydroxyl functionalities, and we proposed previously (19) that Ca^{2+} attached to a carboxylic functionality can induce a proton transfer from T or S to an amide bond (which then becomes protonated), leaving a deprotonated T or S residue that upon collisional activation loses CH_3CHO or CH_2O, respectively. Even for a small model ion-molecule system, *i.e.* $HCOO^-{\bullet\bullet\bullet}Ca^{2+}{\bullet\bullet\bullet}(H)OCH_2CH_2NH_2$ (which contains a carboxylic functionality, an S hydroxyl group, and an amine group) proton transfer from O to N within the ethanol amine moiety to produce the complexed zwitterion $HCOO^-{\bullet\bullet\bullet}Ca^{2+}{\bullet\bullet\bullet}{}^-OCH_2CH_2NH_3{}^+$ proceeds smoothly and without an energy barrier (supplemental Figs. S3 - S9 and supplemental text). That such a facile proton transfer takes place is evident from the observed intense loss of NH_3 from the starting complex $HCOO^-{\bullet\bullet\bullet}Ca^{2+}{\bullet\bullet\bullet}(H)OCH_2CH_2NH_2$, see supplemental Fig. S9. Thus, the OH group of ethanolamine acts as a proton donor whereas the NH_2 group is the proton acceptor. The above losses of acetaldehyde and formaldehyde are also observed after collisional activation of deprotonated peptides, that is, $[P - H]^-$ (20). We observed that motifs that contain a D and/or E in the vicinity of T and/or S and/or Y show a particularly strong calcium affinity.

Fragmentation efficiency curves were obtained on a MALDI-FTICR mass spectrometer for the reference peptide GGGGDEG, bound to various mono-, di-, and trivalent metal ions and the rates of dissociation were compared with that for the reference protonated peptide; the results are shown in Fig. 1. The *y* axis shows the product/precursor ion intensity (×100) and the *x* axis shows the collision energy in the center-of-mass framework. The monovalent metal ions are attached to the neutral peptide, the divalent metal ions to the singly de-

protonated peptide, and the trivalent metal ion to the doubly deprotonated peptide.

To discuss our methodology for establishing calcium-binding sites in proteins, we designed the following strategy. All examples involve LC-MS/MS experiments on complex protein mixtures. First, a control example is discussed were the calcium-binding site is known, the protein calcyclin. The MS/MS spectrum of the calcium-containing peptide as measured in an LC-MS/MS run from a tryptic digest of trophoblasts cells in pre-eclamptic placenta is shown in Fig. 2 and will be discussed below. Next, an example is discussed that was retrieved from archive material present in our laboratory. This concerns existing LC-MS/MS runs recently published (17) on the developing chicken cardiovascular system for three Hamburger–Hamilton stages (HH26, HH30/31, and HH36) and the three accompanying heart tissue structures, namely great arteries, ventricles, and outflow tract. The MS/MS spectrum of the calcium-containing peptide GYSFVTTAER is given in Fig. 3. A final example concerns a protein (HuD) that is not known to bind calcium. From the retrieved LC-MS/MS run, we could identify one peptide that contained calcium, The MS/MS spectrum of the calcium-containing peptide, together with that of the doubly protonated peptide, is shown in Fig. 4.

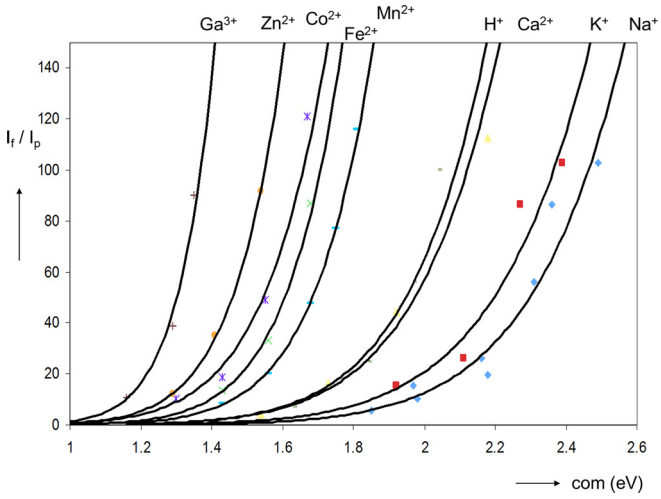

FIG. 1. **Fragmentation efficiency curves for GGGGDEG.** *Y* axis: product ion/precursor ion intensity (×100), *x* axis: center-of-mass frame work. Monitored fragment: b_5 (aspartic cleavage). Collision energy (voltage) = quadrupole voltage + hexapole offset voltage = E_{lab}. $E_{com} = [N/(M+N)]E_{lab}$ [13] where *n* = mass of collision gas (= 40, Ar) and M = precursor ion mass. Note that the calcium-containing peptide fragments at approximately the same rate as the protonated peptide, allowing for the detection of calcium peptides in a routine LC-MS run. Monovalent cations attached to peptide P, divalent cations attached to deprotonated P, and Ga^{3+}attached to doubly deprotonated P.

Detection of calcium-binding sites in peptides or proteins of an enzymatic peptide digest obtained from a complex protein mixture can be achieved by tracing the above calcium-directed dissociations in their MS/MS spectra. This approach would appear particularly appealing because mass spectrometers are routinely coupled to LC systems, enabling identification of large numbers of proteins in complex mixtures. To this end, we defined the following three criteria for high resolution LC-MS data:

1. Deconvoluted to singly charged peptides, a mass signal should be present at 37.9470 Da higher than that of the protonated peptide, compared with 37.9559 Da for the potassium-containing species;

2. Deconvoluted to singly charged peptides, fragments of these peptide species should lose 44 Da if threonine is present or 30 Da if serine is present;

3. The calcium bound and free peptide peaks should be present most preferentially at very similar retention times (we observed that in most cases the retention time was not significantly influenced by calcium coordination on reverse phase C18 columns).

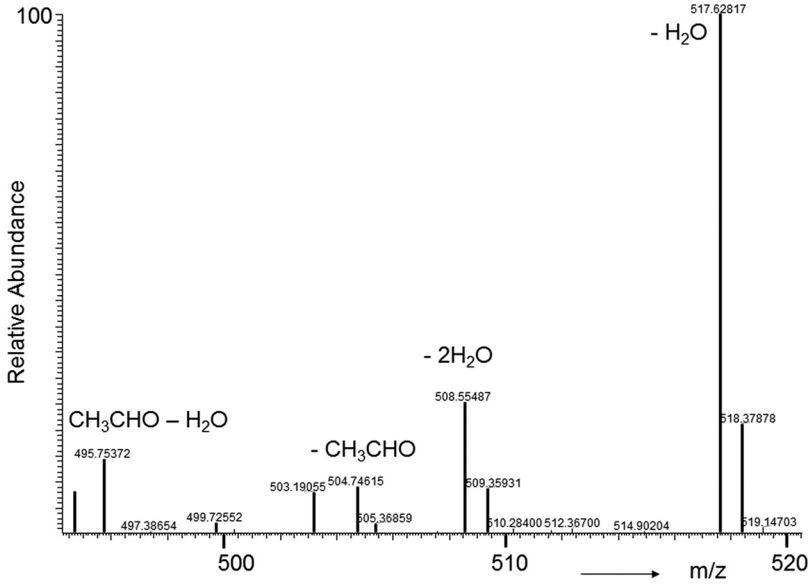

FIG. 2. **LC-MS/MS detection of a calcium-binding peptide (EGDKHTLSK) present in a tryptic digest of calcyclin (S100A6).** Clearly visible are the peaks for loss of CH_3CHO and for the consecutive losses of H_2O and CH_3CHO.

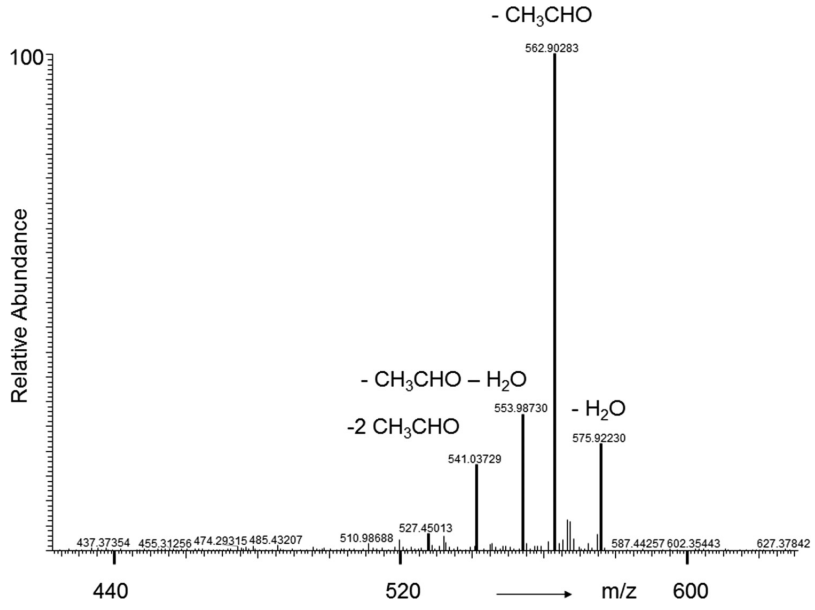

FIG. 3. **LC-MS/MS detection of a calcium-binding peptide (GYSFVTTAER) belonging to the protein α-cardiac actin.** Note the base peak for loss of CH_3CHO.

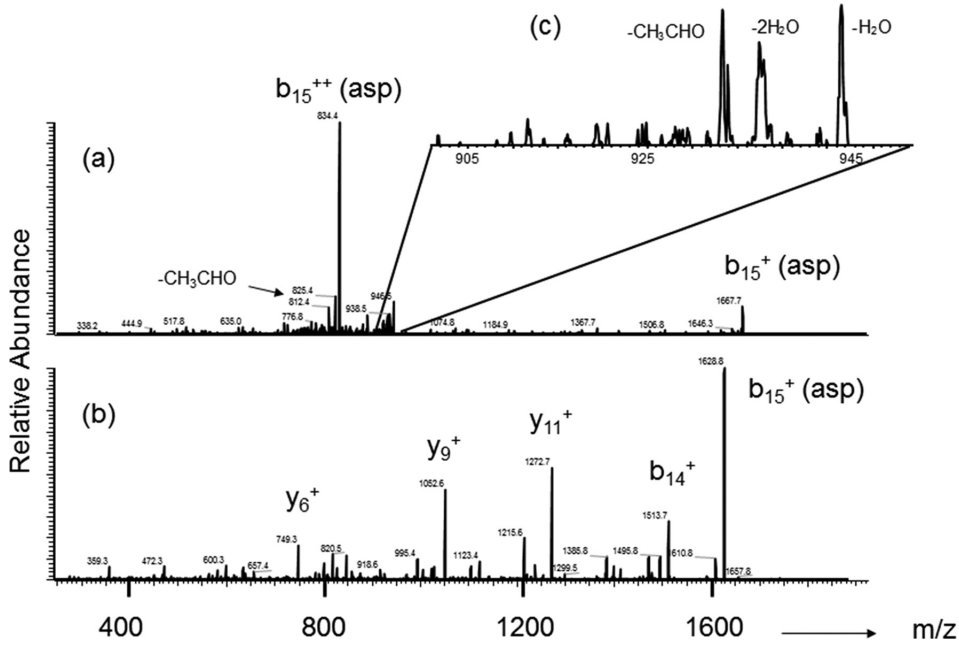

FIG. 4. **LC-MS/MS detection of a calcium-binding peptide (ITGQSLGYGFNYIDPK) in a HuD trypsin digest.** *A*, MS/MS of P + Ca^{2+}; *B*, MS/MS of PH_2^{2+} showing b- and y-fragments but no loss of CH_3CHO; *C*. detail from *A*, showing loss of CH_3CHO.

DISCUSSION

In the mass spectrometer, a particular peptide ion is induced to dissociate by energization using, for example, collisions with a noble gas. Because larger peptide ions have more vibrational degrees of freedom, they require more internal energy to decompose compared with smaller peptide ions, although the dissociating bond may be similar in strength in both cases. Hence, modern mass spectrometers have a feature by which the collision energy is automatically increased as the ion gets larger, thereby allowing for automatic unattended measurements. Because calcium-containing peptides have similar masses as the peptides that do not contain calcium, the automatically chosen collision energies will also be similar. Hence, we need to establish whether the peptide ion without calcium and the calcium-containing peptide ions fragment at the same rate. If not, the optimum collision energy needed to dissociate the calcium-containing peptide ion would have to be evaluated in a separate experiment, leading to a more complicated experimental setup. To ascertain such effects, fragmentation efficiency curves were obtained on our MALDI-FTICR mass spectrometer for a reference peptide GGGGDEG bound to various mono-, di-, and

trivalent metal ions, and the rates of dissociation were compared with that for the reference protonated peptide; see Fig. 1. From theses high-resolution fragmentation efficiency curves, it can be concluded that the $[P_1 - H + Ca]^+$ ions fragment at a much faster rate than the $[P_1 + K]^+$ ions but at a rate similar to the $[P_1 + H]^+$ ions. This is a significant finding for two reasons: (1) Any interference of $[P_1 - H + Ca]^+$ ions by $[P_1 + K]^+$ ions is not seen because $[P_1 + K]^+$ ions do not dissociate at these internal energies; (2) it is not necessary to vary the collision energy to observe the calcium-directed fragmentations and this observation results in a significant simplification of the experimental approach. It is not necessary to manually adjust the collision energy by an *a priori* unknown amount. Perhaps more importantly, because no adjustment of the mass spectrometer is required, our method can be applied to existing, dormant high-resolution MS data files; see below. In addition, it was found that the $[P_1 + H]^+$ ions do not eliminate CH_3CHO from the T residue, and so there will be no interference from any other $[P_2 + H]^+$ ions co-eluting with and having the same exact mass as $[P_1 - H + Ca]^+$. The results presented in Fig. 1 also indicate that if other row 4 metals need to be detected attached to a peptide, for example Zn^{2+}, the collision energy needs to be reduced significantly.

First, as a control experiment, a pure calcium-bound protein with known calcium-binding sites (calcyclin) was investigated as a test case of our approach. Calcyclin (S100-A6), a member of the S100 family of Ca^{2+}-binding proteins that are highly homologous to acidic calcium-binding proteins containing two EF-hand motifs. Calcyclin is elevated in trophoblasts cells in pre-eclamptic placenta (21, 22). Pre-eclampsia is a disease with high protein concentrations in urine and high blood pressure, resulting in a high mortality and morbidity in pregnant women. From the LC-MS run, we could, using criteria 1 and 2, trace one known (20) calcium-containing sequence in calcyclin, (R)EGDKHTLSK(K). The partial MS/MS spectrum of this peptide with Ca^{2+} is given in Fig. 2, and it can be seen that losses of one and two water molecules occur but also loss of CH_3CHO from $[P + Ca]^{2+}$ and from the $[P + Ca - H_2O]^{2+}$ product ion, showing that calcium is present in this domain. This sequence was previously confirmed by x-ray crystallography (23) to be one of the calcium-binding sites of calcyclin (SGREGDKHTLSKKE). This demonstrates that the novel LC-MS/MS method is capable of identifying calcium-binding sites from available data files. The concentration of the calcyclin sample was 1 pmol/μl, and for this concentration, the calcium-binding peptide could easily be detected from the resulting LC-MS/MS collision-induced dissociation (CID) spectra.

A second example concerns a published proteomics study (17) by us a few years ago on the developing chicken cardiovascular system for three Hamburger–Hamilton stages (HH26, HH30/31, and HH36) and the three accompanying heart tissue structures, namely great arteries, ventricles, and outflow tract. In this study, a combination of one-dimensional gel separation, nanoLC separation, and MS was used. A protein abundantly formed in the ventricles at the late HH36 stage was α-cardiac actin, and it is known that actin filaments are severed and capped by gelsolin in a Ca^{2+}-dependent manner. From the retrieved LC-MS run, using criteria 1 and 2, we traced a sequence in α-cardiac actin, *viz*. GYSFVTTAER that contains calcium. The MS/MS spectrum of this peptide + Ca^{2+} is given in Fig. 3, and it can be seen that this spectrum is dominated by loss of CH_3CHO from a T residue, showing that calcium is present in this peptide. Loss of an additional acetaldehyde molecule is detected from the second T residue.

A third example of an LC-MS calcium-binding site determination is provided by the analysis of a tryptic digest of the HuD protein, leading to a mixture of 23 peptides corresponding to 73% coverage. HuD belongs to a family of neuronal RNA-binding proteins that contain two N-terminal RNA binding domains linked by a stringer to a third RNA-binding domain (24). The HuD proteins are highly homologous to the *Drosophila* protein Elav that is critical for the nervous development of the fly. Although its exact function is unknown, HuD is critical for the normal development of the mammalian nervous system during embryogenesis and it might also be involved in synaptic remodeling (25). In addition, the Elav family is involved in oncogenesis (26). Postacquisition MS analysis revealed two peptides that, according to criteria 1 and 3, are likely to bind calcium. These are the tryptic fragments NCPSPMQTGATTDDSK (N36-K51) and ITGQSLGYGFVNYIDPK (I88-K104). These calcium-containing fragments $[P + Ca]^{2+}$ are present at 1% of the $[P + 2H]^{2+}$ intensity (no extra calcium was added in these experiments). In Fig. 4*B*, the MS/MS spectrum of the $[P + 2H]^{2+}$ of the fragment ITGQSLGYGFNYIDPK is given. An extended series of b- and y ions are seen, with the most intense peak for b_{15}^+ corresponding to the aspartic acid side chain cleavage (19, 27). No loss of acetaldehyde could be detected from the parent ion or from any of its product ions. In contrast, for $[P + Ca]^{2+}$ (Fig. 4*A*), the only backbone fragment corresponds to the aspartic cleavage product b_{15}^{2+} ions, *m/z* 834.4 (also present as b_{15}^+ at m/z 1667.7). As can be seen from Fig. 4*C*, loss of acetaldehyde can be observed from the parent ion for $[P + Ca]^{2+}$ as well as from its b_{15}^{2+} ion (The CID spectra in Figs 4*A* and 4*B* were obtained from a standard automated run at the same collision energies). The fulfillment of criteria 1, 2, and 3 demonstrates that the peptide ITGQSLGYGFVNYIDPK corresponding to site 88–104 in the HuD protein contains calcium. Similar experiments revealed losses of CH_3CHO from the $[P + Ca]^{2+}$ ion from NCPSPMQTGATTDDSK.

The function of the calcium that adhered specifically to the HuD protein is unknown. We are currently investigating if, for this protein, calcium binding is changed in tumors.

The three examples show that it is possible to identify yet unknown and known calcium-binding domains in proteins using existing high-resolution MS data files.

In cases where digestion with trypsin leads to a weak signal or to no signal for a peptide, calcium binding may not be detected. This could be the case with the sequence GFGFVTMTNYDEAAMAIASLNGYR, which in our LC-MS run was triggered only once and is thus formed in a minor amount. This peptide contains the fragment TNYDE, which in theory could bind calcium, but this free peptide is detected at a relatively low level, precluding the detection of the corresponding calcium-containing analog.

Using NMR spectroscopy, we studied the calcium-binding site of one of our model compounds, GTNYDEG, in solution (supplemental Fig. S10). TOCSY and NOESY spectra were used to assign protons of the peptide GTNYDEG in presence of calcium formate. The formate proton is evident at 8.4 ppm. Near the T methyl signal, an unidentified methyl group is present. Another group of unidentified protons is visible around 3.5–4.0 ppm. The addition of calcium formate causes spectral changes. Major shifts to lower chemical shifts occur for G7-H, G7-QA, D5-H, and E6-QG suggest that calcium binds to the C terminus, to D5, and the E6 side chain. Minor changes to higher chemical shifts are found for T2-H, T2-HA, T2-HB (and also the N3-side chain HD21) and so the T residue is influenced by coordination. The observation that Ca^{2+} binds to D, in addition to binding to the C terminus, and that the T is part of the coordination is in agreement with the findings from MS, namely that Ca^{2+} binds to D and is able, in the mass spectrometer, to expel a proton from the T residue.

CONCLUSION

We have shown that specific calcium-binding sites (motifs) in peptides and proteins can be identified from LC-MS/MS data obtained from complex protein samples. Tracking the calcium-binding peptide part in the calcium-bound proteins according to the proposed criteria (also applicable in Selective reaction monitoring (SRM) techniques) can lead to more selective and sensitive detection of calcium-bound proteins in complex matrices as well as to the determination of the calcium-binding site in the protein.

The approach is applicable to existing high-resolution MS data files. However, the method is dependent on sensitivity, especially when low abundant proteins are concerned or when the proteolytic peptides are not present at sufficient level in the digested material (the recovery for enzymatic digestion is rarely 100%). We have found that in such cases, a peak for a calcium-containing peptide may well be present, but the peak is not sufficiently intense to trigger the recording of an MS/MS spectrum. In such cases, the LC run has to be repeated but now with an appropriate inclusion mass list. Alternatively, sensitivity may be enhanced by changing, for example, the elution conditions of the nano liquid chromatograph. We are currently identifying parameters that could increase this sensitivity of the method by, for instance, adding Ca^{2+} in the elution fluid or use of more sensitive high-resolution mass spectrometers. We will report on these matters in due course. However, it can already be concluded that our method constitutes a general biochemical approach to define calcium-binding sites in proteins by MS.

[S] This article contains supplemental Figs. S1 to S10 and supplemental Information.

** To whom correspondence should be addressed: Department of Neurology, Laboratory of Neuro-Oncology, Erasmus Medical Center, P.O. Box 2040, 3000 CA, Rotterdam, The Netherlands. Tel.: 31-107044522; Fax: 31-107044365; E-mail: p.burgers@erasmusmc.nl.

† Deceased. The authors fondly remember Mario Ursem as a passionate person and friend interested in research and in the researchers themselves. In particular, the exploration and discovery of new chromatography materials was one of his great achievements.

‡‡ Both authors have contributed equally to this work.

REFERENCES

1. Clapham, D. E. (2007) Calcium signaling. *Cell* **131,** 1047–1058
2. Carafoli, E. (2002) Calcium signaling: A tale for all seasons. *Proc. Natl. Acad. Sci. U.S.A.* **99,** 1115–1122
3. Yao, R., Davidson, D. D., Lopez-Beltran, A., MacLennan, G. T., Montironi, R., and Cheng, L. (2007) The S100 proteins for screening and prognostic grading of bladder cancer. *Histol. Histopathol.* **22,** 1025–1032
4. Pan, Y. R., Lou, Y. C., Seven, A. B., Rizo, J., and Chen, C. (2011) NMR structure and calcium-binding properties of the tellurite resistance protein TerD from *Klebsiella pneumoniae*. *J. Mol. Biol.* **405,** 1188–1201
5. Bryce, D. L. (2010) Calcium binding environments probed by Ca-43 NMR spectroscopy. *Dalton Trans.* **39,** 8593–8602
6. Bart, J., Janssen, J. W., van Bentum, P. J., Kentgens, A. P., and Gardeniers, J. G. (2009) Optimization of stripline-based microfluidic chips for high-resolution NMR. *J. Magn. Reson.* **201,** 175–185
7. Yates, J. R., Ruse, C. I., and Nakorchevsky, A. (2009) Proteomics by mass spectrometry: Approaches, advances, and applications. *Annu. Rev. Biomed. Eng.* **11,** 49–79
8. Walsh, G. M., Rogalski, J. C., Klockenbusch, C., and Kast, J. (2010) Mass spectrometry-based proteomics in biomedical research: Emerging technologies and future strategies. *Expert Rev. Mol. Med.* **12,** 1–28
9. McDonald, L., Robertson, D. H., Hurst, J. L., and Beynon, R. J. (2005) Positional proteomics: Selective recovery and analysis of N-terminal proteolytic peptides. *Nat. Methods* **2,** 955–957
10. Ruttink, P. J., Dekker, L. J., Luider, T. M., and Burgers, P. C. (2012) Complexation of divalent metal ions with diols in the presence of anion auxiliary ligands: Zinc-induced oxidation of ethylene glycol to glycolaldehyde by consecutive hydride ion and proton shifts. *J. Mass Spectrom.* **47,** 869–874
11. Suckau, D., Resemann, A., Schuerenberg, M., Hufnagel, P., Franzen, J., and Holle, A. (2003) A novel MALDI LIFT-TOF/TOF mass spectrometer for proteomics. *Anal. Bioanal. Chem.* **376,** 952–965
12. van Kampen, J. J., Burgers, P. C., de Groot, R., Gruters, R. A., and Luider, T. M. (2011) Biomedical application of MALDI mass spectrometry for small-molecule analysis. *Mass Spectrom. Rev.* **30,** 101–120
13. Laskin, J., and Futrell, J. H. (2003) Collisional activation of peptide ions in FT-ICR mass spectrometry. *Mass Spectrom. Rev.* **22,** 158–181
14. Frisch, M. J. T., G. W., Schlegel, H. B., Scuseria, G. E., Robb, M. A., Cheeseman, J. R., Montgomery, Jr., J. A., Vreven, T., Kudin, K. N., Burant, J. C., Millam, J. M., Iyengar, S. S., Tomasi, J., Barone, V., Mennucci, B., Cossi, M., Scalmani, G., Rega, N., Petersson, G. A., Nakatsuji, H., Hada, M., Ehara, M., Toyota, K., Fukuda, R., Hasegawa, J., Ishida, M., Nakajima, T., Honda, Y., Kitao, O., Nakai, H., Klene, M., Li, X., Knox, J. E., Hratchian, H. P., Cross, J. B., Bakken, V., Adamo, C., Jaramillo, J., Gomperts, R., Stratmann, R. E., Yazyev, O., Austin, A. J., Cammi, R., Pomelli, C., Ochterski, J. W., Ayala, P. Y., Morokuma, K., Voth, G. A., Salvador, P., Dannenberg, J. J., Zakrzewski, V. G., Dapprich, S., Daniels, A. D., Strain, M. C., Farkas, O., Malick, D. K., Rabuck, A. D., Raghavachari, K., Foresman, J. B., Ortiz, J. V., Cui, Q., Baboul, A. G., Clifford, S., Cioslowski, J., Stefanov, B. B., Liu, G., Liashenko, A., Piskorz, P., Komaromi, I., Martin, R. L., Fox, D. J., Keith, T., Al-Laham, M. A., Peng, C. Y., Nanayakkara, A., Challacombe, M., Gill, P. M. W., Johnson, B., Chen, W., Wong, M. W., Gonzalez, C., and Pople, J. A. (2004)

Gaussian 03, Revision C. 02, Gaussian, Inc., Wallingford CT
15. Becke, A. D. (1993) Density-functional thermochemistry. III. The role of exact exchange. *J. Chem. Phys.* **98,** 5648–5652
16. Lee, C. Y., W., and Parr, R. G. (1998) Development of the Colle–Salvetti correlation-energy formula into a functional of the electron density. *Phys. Rev. B* **37,** 785–789
17. Bon, E., Steegers, R., Steegers, E. A., Ursem, N., Charif, H., Burgers, P. C., Luider, T. M., and Dekker, L. J. (2010) Proteomic analyses of the developing chicken cardiovascular system. *J. Proteome Res.* **9,** 268–274
18. VanDuijn, M. M., Dekker, L. J., Zeneyedpour, L., Smitt, P. A., and Luider, T. M. (2010) Immune responses are characterized by specific shared immunoglobulin peptides that can be detected by proteomic techniques. *J. Biol. Chem.* **285,** 29247–29253
19. Jobst, K. J., Terlouw, J. K., Luider, T. M., and Burgers, P. C. (2008) On the interaction of peptides with calcium ions as studied by matrix-assisted laser desorption/ionization Fourier transform mass spectrometry: Towards peptide fishing using metal ion baits. *Anal. Chim. Acta* **627,** 136–147
20. Boontheung, P., Alewood, P. F., Brinkworth, C. S., Bowie, J. H., Wabnitz, P. A., and Tyler, M. J. (2002) Negative ion electrospray mass spectra of caerulein peptides: an aid to structural determination. *Rapid Commun. Mass Spectrom.* **16,** 281–286
21. Guzel, C., Ursem, N. T., Dekker, L. J., Derkx, P., Joore, J., van Dijk, E., Ligtvoet, G., Steegers, E. A., and Luider, T. M. (2011) Multiple reaction monitoring assay for pre-eclampsia related calcyclin peptides in formalin fixed paraffin embedded placenta. *J. Proteome Res.* **10,** 3274–3282
22. Schol, P. B. B., Güzel, C., Steegers, E. A. P., de Krijger, R. R., and Luider, T. M. (2014) Trophoblast calcyclin is elevated in placental tissue from patients with early pre-eclampsia. *Preg. Hyper.: An Int. J. Women's Card. Health* **4,** 7–10
23. Otterbein, L. R., Kordowska, J., Witte-Hoffmann, C., Wang, C. L., and Dominguez, R. (2002) Crystal structures of S100A6 in the Ca(2+)-free and Ca(2+)-bound states: the calcium sensor mechanism of S100 proteins revealed at atomic resolution. *Structure* **10,** 557–567
24. Szabo, A., Dalmau, J., Manley, G., Rosenfeld, M., Wong, E., Henson, J., Posner, J. B., and Furneaux, H. M. (1991) HuD, a paraneoplastic encephalomyelitis antigen, contains RNA-binding domains and is homologous to Elav and Sex-lethal. *Cell* **67,** 325–333
25. Deschenes-Furry, J., Perrone-Bizzozero, N., and Jasmin, B. J. (2006) The RNA-binding protein HuD: A regulator of neuronal differentiation, maintenance and plasticity. *BioEssays* **28,** 822–833
26. Filippova, N., Yang, X., Wang, Y., Gillespie, G. Y., Langford, C., King, P. H., Wheeler, C., and Nabors, L. B. (2011) The RNA-binding protein HuR promotes glioma growth and treatment resistance. *Mol. Cancer Res.* **9,** 648–659
27. Rozman, M. (2007) Aspartic acid side chain effect-experimental and theoretical insight. *J. Am. Soc. Mass Spectrom.* **18,** 121–127